

A novel derivative of Genistein inhibits proliferation of ovarian cancer HO-8910 cells by regulating reactive oxygen species*

Yanping Gao¹, Zhiyong Dong², Jun Bai^{1,3} (✉)

¹ Department of Gynecology, The First People's Hospital of Datong (Women and Children's Hospital of Shanxi Datong University), Datong 037000, China

² Department of Gynecology, The First Affiliated Hospital of Jinan University, Guangzhou 510630, China

³ Institute of Oncology, Shanxi Datong University, Datong 037000, China

Abstract

Objective To investigate the anticancer effect of a novel derivative of genistein (5-hydroxy-4'-nitro-7-propionyloxy-genistein, HNPG) on human ovarian cancer HO-8910 cells and its possible molecular mechanism.

Methods HO-8910 cells were cultured *in vitro*, and the inhibitory effect of HNPG on proliferation was determined using MTT [3-(4,5-dimethylthiazol-2-yl)-2,5-diphenyltetrazolium bromide] assay. The effect of HNPG on inducing apoptosis was examined using FCM with Annexin V-FITC and propidium iodide staining. The effect of HNPG on regulating reactive oxygen species (ROS) was measured using FCM with 2',7'-dichlorodihydro-fluorescein diacetate staining. The effect of HNPG on modulating mitochondrial membrane potential (MMP) was determined using FCM with lipophilic cationic dye 2 (6 Amino 3 imino 3H xanthen 9 yl) benzoic acid methyl ester (Rh123) staining. The bioactivity of superoxide dismutase (SOD) and catalase (CAT) and the content of glutathione (GSH) and malondialdehyde (MDA) were detected using enzyme-linked immunosorbent assay. The related apoptotic proteins, including bcl-2, bax, cyt-c, and cleaved-caspase-3, were assessed using western blotting.

Results HNPG exhibited dramatic antitumor activity against HO-8910 cells *in vitro*, inhibited proliferation, and induced apoptosis in a time- and dose-dependent manner. These effects were accompanied by reduced bioactivity of SOD and CAT, reduced GSH content, and enhanced MDA content. Simultaneously, the amount of ROS was increased and the level of MMP was reduced, along with upregulation of mitochondrial apoptosis pathway-related proteins, bax, cyt-c, and cleaved-caspase-3; bcl-2 protein was downregulated.

Conclusion HNPG inhibited proliferation of human ovarian cancer HO-8910 cells *in vitro*, which might be related to decreased bioactivity of SOD and CAT. HNPG also reduced GSH content, which resulted in ROS accumulation in cells, damaged the integrity of mitochondrial membrane, and induced cell apoptosis.

Key words: ovarian cancer; 5-hydroxy-4'-nitro-7-propionyloxy-genistein; reactive oxygen species; proliferation; apoptosis

Received: 10 September 2022

Revised: 30 November 2022

Accepted: 15 December 2022

Chemotherapy plays an extremely important role in the treatment of ovarian cancer; postoperative chemotherapy and preoperative neoadjuvant chemotherapy have greatly improved patient prognosis in recent years [1]. Not only can chemotherapy kill residual cancer foci, control recurrence, alleviate symptoms, prolong survival time, and reduce cancer volume to create satisfactory conditions for surgeons, it also serves as the main treatment for patients who cannot tolerate surgery [2].

Therefore, the development of new anticancer drugs with more anticancer effects and fewer side-effects has become one of the hot spots in clinical research [1, 2].

It was reported that Genistein (GEN) caused extensive pharmacological effects and could inhibit proliferation and induce apoptosis of cancer cells, but its clinical application was limited due to its poor solubility and low bioavailability [3]. However, the solubility and bioavailability of GEN could be improved, and

✉ Correspondence to: Jun Bai. Email: baijunjinanu@163.com

* Supported by a grant from the Scientific Research Project of Shanxi Provincial Health Commission (No. 2021166).

© 2019 Huazhong University of Science and Technology

the antitumor activity increased through chemical modification of its structure [4]. 5-hydroxy-4'-nitro-7'-propionyloxy-genistein (HNPG) is a novel derivative of GEN, which includes nitro-4' and propionyloxy-7' in the parent nucleus of GEN [5]. HNPG reportedly possesses more anticancer activity than GEN, though its effect against ovarian cancer and its molecular mechanism have not yet been reported [6].

This study examined the inhibitory effect of HNPG on the proliferation of ovarian cancer HO-8910 cells, further investigated its possible molecular biological mechanism, and provided an experimental basis for the clinical treatment of ovarian cancer with HNPG.

Materials and methods

Cells and reagents

Human ovarian cancer HO-8910 cells were purchased from the China Center for Type Culture Collection and cultured in Dulbecco's modified Eagle medium (DMEM) medium containing 10% fetal bovine serum at 37 °C with 5% CO₂ and saturated humidity. HNPG (molecular formula C₁₈H₁₃O₇N, molecular weight 355, faint yellow powder, 98% purity) was synthesized by Professor Jin Yongsheng (Biochemical Laboratory of Naval Military Medical University of China). Primary antibodies of bcl-2 (A00040-1), bax (A00183), cyt-c (BA0774), cleaved caspase-3 (BM3937), and glyceraldehyde-3-phosphate dehydrogenase (GAPDH) (A00227-1) were purchased from Boster Biotechnology Co., LTD. The determination kits of reactive oxygen species (ROS) (E004-1-1), superoxide dismutase (SOD) (A001-3), catalase (CAT) (A007-1-1), glutathione (GSH) (A006-1), and malondialdehyde (MDA) (A003-4) were bought from Nanjing Jiancheng Institute of Biology. Annexin V-FITC apoptosis detection kit (C0162) and mitochondrial membrane potential detection kit (C2006) were obtained from Shanghai Beyond Biological Company. MTT (C0009), penicillin-streptomycin solution (C0022), pancreatic protein digestive enzyme (C0205), and bicinchoninic acid (BCA) protein concentration determination kit (P0012S) were purchased from Beyotime Biotechnology Institute. Cell lysate (ARAR0107) and standard fetal bovine serum (PYG0001) were purchased from Boster Biotechnology LTD.

MTT analysis

HO-8910 cells in logarithmic growth phase were plated on a 96-well culture plate at a density of 5,000/well for 24 h. After the cells completely adhered to the culture plate, different concentrations of HNPG (0.625, 1.25, 2.5, 5, 10, 20, 40 μmol/L) were added to each well for 48 h. The inhibitory effect on proliferation of HO-8910 cells was detected, and the optimal concentration and action

time associated with optimal bioactivity were selected and administrated for subsequent experiments. The cells were incubated using DMEM medium containing cisplatin 5 μmol/L, GEN 160 μmol/L, or HNPG (5, 10, or 20 μmol/L) for 48 h. The culture medium was then removed, and 5 mg/L MTT was added to each well for further incubation for 4 h. Next, the MTT suspension was removed, and 100 μL Dimethyl sulfoxide (DMSO) was added. The wavelength of 570 nm was selected to detect the optical density (model: ELX-800 Type). Cell proliferation inhibition rate (IR) was calculated as follows: IR = (1 - mean of experimental group A / mean of blank control group A) × 100%. IC₅₀ was obtained using the improved Koch method. The experiment was repeated three times, and the mean values were used for statistical analysis.

FCM of annexin V-FITC (AV) and propidium iodide (PI) staining

HO-8910 cells in logarithmic phase were cultured for 24 h to ensure that the cells completely adhered to the bottle bottom. The culture medium was renewed with EMEM medium containing DDP (5 μmol/L), GEN (160 μmol/L), or HNPG (2.5, 5, or 10 μmol/L). After 48 h, the treatment media were discarded and the cells were cleaned twice with PBS. The cells were digested with 0.25% trypsin and beaten into single cell suspension. The suspended cells were centrifuged at 2,000 rpm for 5 min, and the supernatant was discarded. The cellular precipitate was resuspended in 1 mL 50 mmol AV and 50 mmol PI solution, incubated at 37 °C for 30 min in a dark room, then washed with serum-free DMEM solution three times. The apoptotic cells were measured using FCM with an excitation wavelength of 488 nm and an emission wavelength of 530 nm. The experiment was conducted three times, and the average values were taken for statistical analysis.

FCM of DCFH-DA staining

HO-8910 cells in logarithmic phase were incubated and completely adhered to the bottle bottom for 24 h. The culture medium was changed to fresh DMEM medium containing DDP (5 μmol/L), GEN (160 μmol/L), or HNPG (2.5, 5, 10 μmol/L), and the cells continued to incubate for 48 h. The treatment media were discarded and the bottle bottom was cleaned twice with PBS. The cells were digested with 0.25% trypsin and resuspended in culture medium. The cellular suspension was centrifuged at 2,000 rpm for 5 min, and the supernatant was discarded. The cellular precipitate was suspended in 1 mL 50 mmol 2',7'-dichlorodihydrofluorescein diacetate (DCFH-DA) solution, and incubated at 37 °C for 30 min in a dark room, then washed three times with serum-free DMEM solution to remove DCFH-DA that did not enter

the cells. The cells were passed through a 40 μm filter. The fluorescence intensity of DCFH-DA was measured using FCM with an excitation wavelength of 488 nm and emission wavelength of 530 nm. The experiment was performed three times, and the average values were adopted for statistical analysis.

FCM of Rhodamine 123 staining

HO-8910 cells in logarithmic phase were cultured and completely adhered to the bottle bottom for 24 h. The culture medium was replaced with new DMEM medium containing DDP (5 $\mu\text{mol/L}$), GEN (160 $\mu\text{mol/L}$), or HNPG (2.5, 5, or 10 $\mu\text{mol/L}$). The cells continued to incubate for 48 h; then the culture medium was discarded, and the bottle bottom was cleaned twice with PBS. The cells were digested with 0.25% trypsin and resuspended. The cell suspension was centrifuged at 2,000 rpm for 5 min, and the supernatant was discarded. The cell precipitate was suspended in 500 μL Rh123 solution (final concentration 5 $\mu\text{g/mL}$), and incubated at 37 $^{\circ}\text{C}$ for 30 min in a dark room. The cells were washed three times with serum-free DMEM solution and two times with PBS, then passed through a 40 μm filter. The fluorescence intensity of Rh123 was measured using FCM with an excitation wavelength of 475 nm and emission wavelength of 525 nm. The experiment was repeated three times, and the average values were calculated for statistical analysis.

Enzyme-linked immunosorbent assay (ELISA) method

HO-8910 cells in logarithmic phase were incubated for 24 h until they completely adhered to the bottle bottom. The culture medium was changed with new DMEM medium containing DDP (5 $\mu\text{mol/L}$), GEN (160 $\mu\text{mol/L}$), or HNPG (2.5, 5, or 10 $\mu\text{mol/L}$), and the cells continued to incubate for 48 h. The cells were digested with 0.25% trypsin and resuspended. The cellular suspension was centrifuged at 800 rpm for 5 min, the supernatants were discarded, and the cell precipitates were suspended twice with ice PBS. As a final step, the cellular precipitate was lysed using cell lysis solution for 30 min, and the supernatant was centrifuged at 1,200 rpm at 4 $^{\circ}\text{C}$ for 10 min. Protein density in the supernatant was determined with a BCA protein quantitation kit. In accordance with the appropriate kit instructions, SOD activity, CAT activity, GSH contents, and MDA contents were measured at 550 nm, 405 nm, 420 nm, and 532 nm, respectively. The calculation formulas of enzyme activity/content were as follows: Total SOD activity (U/mg) = $([\text{OD}_{\text{control group}} - \text{OD}_{\text{experimental group}}] / \text{OD}_{\text{control group}}) / 50\% \times (V_{\text{total reaction liquid}} / V_{\text{sample}}) / C_{\text{protein}}$; CAT activity (U/mgprot) = $(\text{OD}_{\text{control group}} - \text{OD}_{\text{experimental group}}) \times 271 \times 1 / (60 \times V_{\text{sample}}) / C_{\text{protein}}$ (gprot/mL); GSH content (mgGSH/gprot) = $([\text{OD}_{\text{Determinationvalue}} - \text{OD}_{\text{blankvalue}}] / [\text{OD}_{\text{standard value}} - \text{OD}_{\text{blank}}$

$\text{value}]) \times C_{\text{standard concentration}} (20 \times 10^{-3} \text{ mmol/L}) \times W_{\text{molecular weight (307)}} \times R_{\text{dilution ratio of sample before test}} / C_{\text{homogenate protein(gprot/l)}}$; MDA content (nmol/mgprot) = $([\text{OD}_{\text{experimental group}} - \text{OD}_{\text{control group}}] / [\text{OD}_{\text{standard value}} - \text{OD}_{\text{standard value}}]) \times C_{\text{standard product}} / C_{\text{protein content}}$. The experiment was performed three times, and the average values were taken for statistical analysis.

Western blotting assay

HO-8910 cells in logarithmic phase were cultured for 24 h until they completely adhered to the bottle bottom. The culture medium was discarded and new DMEM media with different concentrations of HNPG (2.5, 5, or 10 $\mu\text{mol/L}$) were added for a 48 h incubation. The cells on the bottle bottom were washed three times with ice-cold PBS, and the cell lysis solution was added to extract proteins. A 30 μg sample was separated using sodium dodecyl sulfate-polyacrylamide gel electrophoresis (SDS-PAGE), and the protein was transferred to polyvinylidene fluoride (PVDF) membrane. The protein was blocked with 5% nonfat milk in Tris-buffered saline with Tween-20 (TBST) in a room temperature shaker for 2 h. The primary antibody was incubated at 37 $^{\circ}\text{C}$ for 3 h, and the secondary antibody was incubated at 37 $^{\circ}\text{C}$ for 1 h. The fluorescence of antigen-antibody reactions was stimulated using enhanced chemiluminescent agents, and the film was exposed to the reacting fluorescence. The resulting film image was processed and analyzed using a grayscale scanner. The experiment was repeated three times, and the average values were used for statistical analysis.

Statistical analyses

The data were analyzed using statistical product and service solutions 21.0 software. All experimental data were expressed as mean \pm standard deviation ($\bar{x} \pm s$). Comparisons between the two groups were analyzed using student's *t* test, and multiple groups were analyzed using one-way analysis of variance. $P < 0.05$ indicated statistical differences.

Results

Effect of HNPG on proliferation of HO-8910 cells

The different concentrations of HNPG (0.625, 1.25, 2.5, 5, 10, 20, and 40 $\mu\text{mol/L}$) were administrated to HO-8910 cells for 48 h, and it was found that the cellular proliferation was inhibited in a concentration-dependent manner. The most significant inhibition by HNPG occurred at a concentration between 1.25 and 20 $\mu\text{mol/L}$. Compared with the normal saline (NS) group, the inhibition rates of different concentrations of HNPG were statistically significant ($P < 0.05$), as shown in Fig. 1a. HNPG was found to inhibit the proliferation of HO-

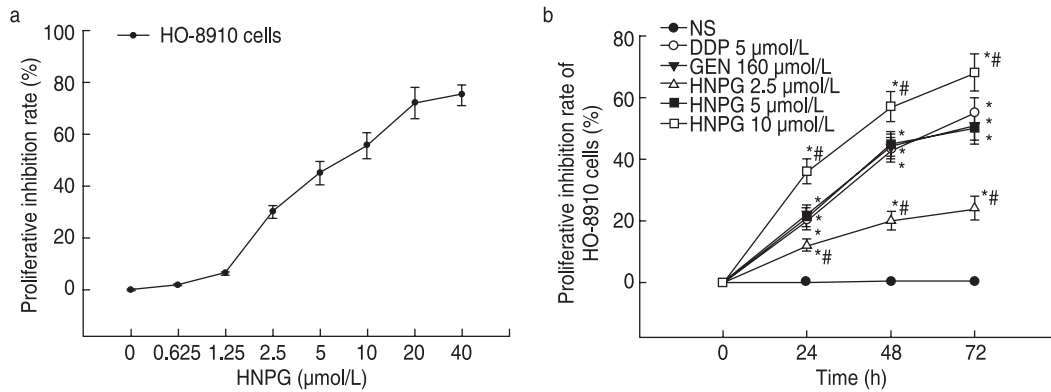


Fig. 1 The inhibitory effect of HNPG on proliferation of HO-8910 cells. (a) The inhibition rate of HO-8910 cells treated with different concentrations of HNPG for 48 h; (b) The inhibition rate of HO-8910 cells treated with different concentrations of HNPG at different times. * $P < 0.05$ vs. the NS group; # $P < 0.05$ vs. the 5 μmol/L DDP group, or 160 μmol/L GEN group

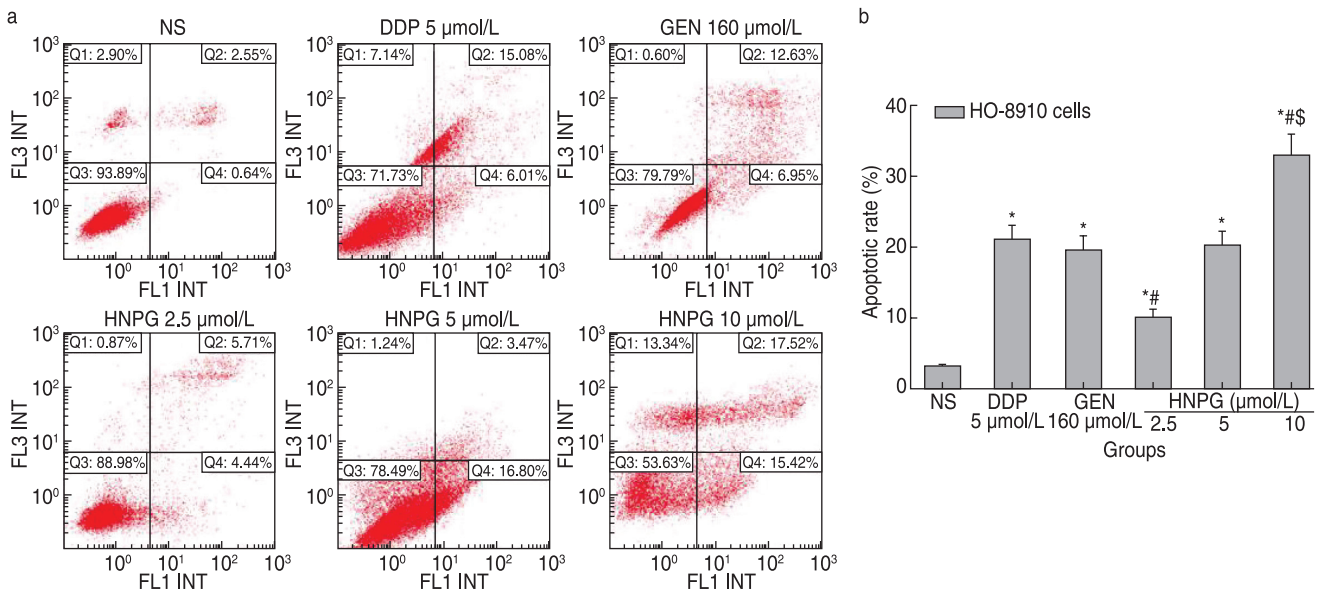


Fig. 2 The effect of HNPG on apoptosis of HO-8910 cells. * $P < 0.05$ vs. the NS group; # $P < 0.05$ vs. 5 μmol/L DDP group, 5 μmol/L HNPG group, or 160 μmol/L GEN group; \$ $P < 0.05$ vs. 5 μmol/L DDP group, 5 μmol/L HNPG group, or 160 μmol/L GEN group

8910 cells in a time-dependent manner. The different groups of HNPG (2.5, 5, and 10 μmol/L) at different time-points (24, 48, and 72 h) showed statistical differences in the inhibition rate of HO-8910 cells ($P < 0.05$), and the IC₅₀ of HO-8910 cells treated with HNPG for 48 h was 4.8 ± 0.6 μmol/L. The inhibitory effect of 5 μmol/L HNPG on the proliferation of HO-8910 cells was similar to 5 μmol/L DDP or 160 μmol/L GEN, and there was no significant difference between the latter two groups ($P < 0.05$) (Fig. 1b).

Effect of HNPG on induced apoptosis of HO-8910 cells

HO-8910 cells in logarithmic phase were cultured with NS, DDP (5 μmol/L), GEN (160 μmol/L), or HNPG

(2.5, 5, and 10 μmol/L) for 48 h. FCM showed that HO-8910 cells underwent apoptosis to varying degrees. The apoptotic rates of NS, DDP (5 μmol/L), GEN (160 μmol/L), and HNPG (2.5, 5, and 10 μmol/L) groups were $3.19 \pm 0.42\%$, $21.06 \pm 1.47\%$, $19.65 \pm 1.69\%$, $10.24 \pm 1.13\%$, $20.25 \pm 2.04\%$, and $32.83 \pm 3.12\%$, respectively, and the apoptotic rates of each research group were higher than that of the NS group ($P < 0.05$). There were statistical differences between each concentration of HNPG (2.5, 5, and 10 μmol/L) groups ($P < 0.05$). The apoptotic rate of the 5 μmol/L HNPG group was close to that of the 160 μmol/L GEN or 5 μmol/L DDP groups, and there was no significant difference between the latter two groups ($P > 0.05$), as shown in Fig. 2.

Effect of HNPG on ROS regulation in HO-8910 cells

HO-8910 cells in logarithmic phase were incubated with NS, DDP (5 $\mu\text{mol/L}$), GEN (160 $\mu\text{mol/L}$), or HNPG (2.5, 5, and 10 $\mu\text{mol/L}$) for 48 h. FCM indicated that the fluorescence intensity of DCFH-DA in HO-8910 cells was increased to varying degrees. The fluorescence intensity of the DDP (5 $\mu\text{mol/L}$), GEN (160 $\mu\text{mol/L}$), and HNPG (2.5, 5, 10 $\mu\text{mol/L}$) groups were 0.78 ± 0.08 , 4.45 ± 0.47 , 4.29 ± 0.49 , 2.24 ± 0.13 , 4.38 ± 0.44 , and 6.26 ± 0.52 , respectively, and there were statistical differences between each research group and the NS group ($P < 0.05$). There were also statistically significant differences between the HNPG (2.5, 5, and 10 $\mu\text{mol/L}$) groups ($P < 0.05$). The fluorescence intensity of the 5 $\mu\text{mol/L}$ HNPG group was close to the 160 $\mu\text{mol/L}$ GEN or 5 $\mu\text{mol/L}$ DDP group, and there was no statistical difference between the latter two groups ($P > 0.05$), as shown in Fig. 3.

Effect of HNPG on mitochondrial membrane potential (MMP) adjustment in HO-8910 cells

HO-8910 cells in logarithmic phase were cultured in medium containing NS, DDP (5 $\mu\text{mol/L}$), GEN (160 $\mu\text{mol/L}$), or HNPG (2.5, 5, and 10 $\mu\text{mol/L}$) for 48 h. FCM demonstrated that Rh 123 fluorescence intensity of HO-8910 cells decreased to varying degrees. The fluorescence intensity of the NS, DDP (5 $\mu\text{mol/L}$), GEN (160 $\mu\text{mol/L}$), and HNPG (2.5, 5, 10 $\mu\text{mol/L}$) groups were 10.02 ± 0.86 , 5.5 ± 0.42 , 5.66 ± 0.48 , 8.38 ± 0.63 , 6.16 ± 0.54 , and 2.28 ± 0.12 , respectively, and there were statistical differences compared with the NS group ($P < 0.05$). There were statistically significant differences between each pair of HNPG concentrations ($P < 0.05$). The fluorescence

intensity of the 5 $\mu\text{mol/L}$ HNPG group was analogous to the 160 $\mu\text{mol/L}$ GEN and 5 $\mu\text{mol/L}$ DDP groups, and there was no significant difference between the latter two groups ($P > 0.05$), as shown in Fig. 4.

Effect of HNPG on SOD, CAT, GSH, and MDA modulation in HO-8910 cells

HO-8910 cells in logarithmic phase were incubated with DMEM medium, including DDP (5 $\mu\text{mol/L}$), GEN (160 $\mu\text{mol/L}$), or HNPG (2.5, 5, and 10 $\mu\text{mol/L}$) for 48 h. ELISA assays indicated that SOD and CAT activity were reduced, GSH content was reduced, and MDA content was increased. There was statistical significance compared with the NS group ($P < 0.05$). There were statistical differences in SOD activity, CAT activity, GSH content, and MDA content between any two HNPG groups ($P < 0.05$). SOD/CAT activity in the 5 $\mu\text{mol/L}$ HNPG group was similar to the 160 $\mu\text{mol/L}$ GEN or 5 $\mu\text{mol/L}$ DDP group, and GSH/MDA content in 5 $\mu\text{mol/L}$ HNPG groups were similar to the 5 $\mu\text{mol/L}$ GEN or 5 $\mu\text{mol/L}$ DDP groups, while there was no statistical significance between the latter two groups ($P > 0.05$), as shown in Table 1.

Effect of HNPG on mitochondrial apoptosis pathway-related proteins regulated in HO-8910 cells

Logarithmic proliferating HO-8910 cells were cultured with DMEM medium containing different concentrations of HNPG (2.5, 5, and 10 $\mu\text{mol/L}$) for 48 h, the cellular proteins were extracted, and the average relative gray values of western blots were detected. The expression of bcl-2 protein was downregulated in a concentration-dependent manner, and there was a statistical difference

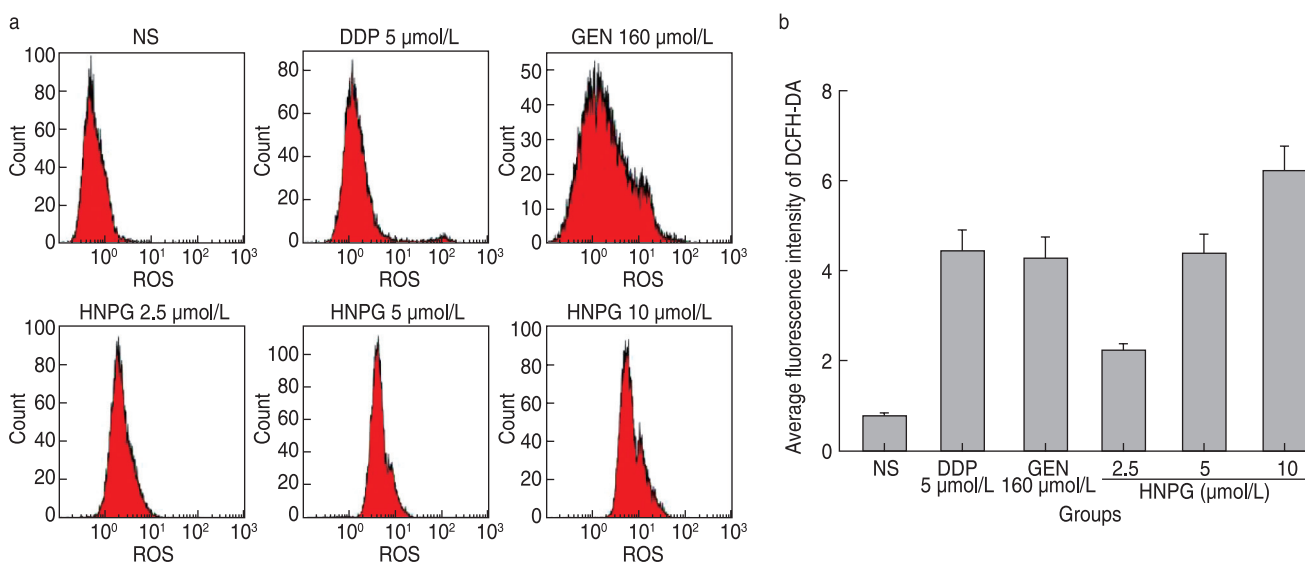


Fig. 3 The effect of HNPG on ROS regulation in HO-8910 cells. * $P < 0.05$ vs. the NS group; # $P < 0.05$ vs. 5 $\mu\text{mol/L}$ DDP group, 5 $\mu\text{mol/L}$ HNPG group, or 160 $\mu\text{mol/L}$ GEN group; § $P < 0.05$ vs. 5 $\mu\text{mol/L}$ DDP group, 5 $\mu\text{mol/L}$ HNPG group, or 160 $\mu\text{mol/L}$ GEN group

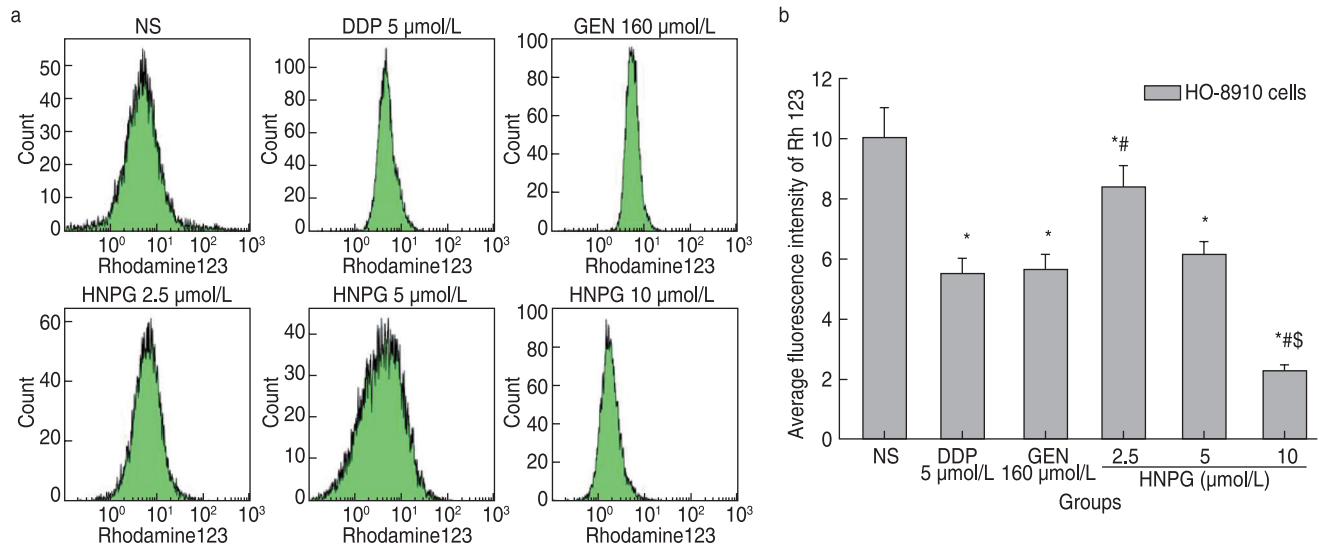


Fig. 4 The effect of HNPNG on MMP adjustment in HO-8910 cells. * $P < 0.05$ vs. the NS group; # $P < 0.05$ vs. 5 $\mu\text{mol/L}$ DDP group, 5 $\mu\text{mol/L}$ HNPNG group, or 160 $\mu\text{mol/L}$ GEN group; § $P < 0.05$ vs. 5 $\mu\text{mol/L}$ DDP group, 5 $\mu\text{mol/L}$ HNPNG group, or 160 $\mu\text{mol/L}$ GEN group

Table 1 Effect of HNPNG on SOD, CAT, GSH and MDA modulation in HO-8910 cells

Groups	SOD (U/mgprot)	CAT (U/mgprot)	GSH (mg/gprot)	MDA (nmol/mgprot)
NS	46.59 \pm 2.21	10.89 \pm 1.12	12.47 \pm 1.07	4.43 \pm 0.27
DDP 5 $\mu\text{mol/L}$	31.08 \pm 1.84*	5.98 \pm 0.12*	6.28 \pm 0.37*	8.54 \pm 0.47*
GEN 160 $\mu\text{mol/L}$	32.90 \pm 3.31#	6.52 \pm 0.09#	6.45 \pm 0.11#	8.76 \pm 0.27#
HNPNG 2.5 $\mu\text{mol/L}$	43.85 \pm 2.04*#	8.65 \pm 0.52*#	9.52 \pm 0.48*#	5.04 \pm 0.41*#
HNPNG 5 $\mu\text{mol/L}$	32.70 \pm 3.06*	6.70 \pm 0.43*	6.97 \pm 0.44*	8.49 \pm 0.31*
HNPNG 10 $\mu\text{mol/L}$	25.72 \pm 3.08*#§	4.18 \pm 0.47*#§	4.46 \pm 0.63*#§	10.62 \pm 0.22*#§

* $P < 0.05$ vs the NS group; # $P < 0.05$ vs 5 $\mu\text{mol/L}$ DDP group, or 5 $\mu\text{mol/L}$ HNPNG group, or 160 $\mu\text{mol/L}$ GEN group; § $P < 0.05$ vs. 5 $\mu\text{mol/L}$ DDP group, or 5 $\mu\text{mol/L}$ HNPNG group, or 160 $\mu\text{mol/L}$ GEN group

compared with the NS group ($P < 0.05$). However, bax, cyt-c, and cleaved caspase-3 proteins were upregulated in a concentration-dependent manner, and there were statistical differences compared with the NS group ($P < 0.05$; Fig. 5).

Discussion

Atypical proliferation is one of the malignant manifestations of cancer; the rapidly and abnormally proliferating cancer cells not only compress, infiltrate, and damage the surrounding tissue, but also cause metastasis. Simultaneously, the cancer cells release harmful substances into the blood, lymph, and tissue fluid, which threaten the regulatory function of the immune system and affect the balance and stability of the internal environment. Therefore, inhibiting proliferation of cancer cells has become one of the key steps in cancer treatment [7]. Apoptosis is a kind of programmed cell death in which signal transduction pathways are initiated by factors originating internally and externally to the

body. Death signals are received by apoptosis-related genes, and various enzymes implementing apoptosis, such as endogenous nuclease and caspase, are synthesized [8]. Apoptosis plays an important role in modern oncology chemotherapy; many chemical medicines exert their antitumor role via induction of tumor cell apoptosis [8]. Chemotherapy remains the most important method to treat ovarian cancer aside from surgery. Chemical medicines, which have entered organisms can kill malignant cells, inhibit cancer cell proliferation, and induce tumor cell apoptosis, thereby playing a crucial role in reducing various damages caused by cancer proliferation and invasion [9, 10]. In this study, we found that HNPNG could inhibit proliferation and induce apoptosis of ovarian cancer HO-8910 cells, with an effect similar to DDP or GEN, suggesting that HNPNG has potential as a chemical substance to treat ovarian cancer. These findings indicate that the possible molecular biological mechanism is worth investigating.

A balanced oxidation-antioxidant enzyme system exists in organisms, which plays an important role in

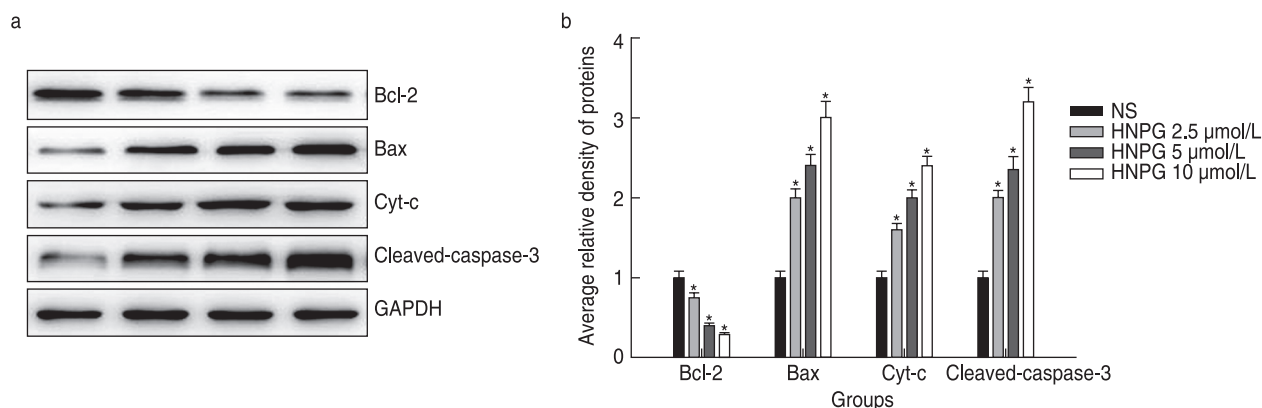


Fig. 5 Effect of HNPG on apoptosis-related protein regulation in HO-8910 cells. * $P < 0.05$ vs. the NS group

maintaining the balance and stability of the internal environment [11]. The antioxidant system includes SOD, CAT, GSH, and other enzymes [11]. SOD is one of most important antioxidant enzymes and can directly withstand oxygen free radicals and ROS in the body; this enzyme can take superoxide anion free radicals as the substrate to catalyze its disproportionation reaction to generate nontoxic oxygen or hydrogen peroxide [12]. CAT is another key enzyme in the defense system, which can effectively catalyze hydrogen peroxide into nontoxic oxygen [13]. GSH can also effectively catalyze hydrogen peroxide into nontoxic oxygen and water [14]. SOD, CAT, and GSH play significant roles in the antioxidant enzyme system. The determination of SOD activity, CAT activity, and GSH content can indirectly reflect the antioxidant capacity of organisms, including oxygen free radicals and purged ROS [15]. Organisms can produce oxygen free radicals or ROS via enzyme systems themselves, which can attack polyunsaturated fatty acids in biofilms, induce lipid peroxidation, and form lipid peroxides, such as MDA; therefore, the amount of MDA can reflect the degree of lipid peroxidation in body, which indirectly indicates the degree of cell damage [16]. In this study, it was found that the content of ROS in HO-8910 cells was improved by HNPG, accompanied by decreased SOD and CAT bioactivity, reduced GSH content, and enhanced MDA content. This suggested that the effect of HNPG on inhibiting proliferation and inducing apoptosis of HO-8910 cells was closely related to the function of the oxidant-antioxidant enzyme system brought down, which led to ROS accumulation in HO-8910 cells and damaged the mitochondrial phospholipid membrane.

Mitochondria are vital organelles for cellular oxidative phosphorylation, and transformation holes jointly assembled by bcl-2 and bax proteins in the phospholipid bilayer of mitochondria maintain the normal communication between the intra and extra-mitochondrial environments [17, 18]. When the mitochondrial membrane is damaged, the substances in the

mitochondrion spill out, which not only directly reduces MMP, but also initiates a cellular apoptotic reaction [19]. When MMP is downregulated and mitochondrial substances leak, a vicious cycle develops that promotes the initiation of cellular apoptosis. Simultaneously, bcl-2 and/or bax proteins are abnormally regulated and their ratio unbalanced, which will also lead to downregulation of MMP and cause mitochondrial substances to spill over, including cyt-c, apoptosis inductive factor, or apoptosis protease-activating factor. Once the mitochondrial substances are released into the cytoplasm, the caspase family cascade reaction is activated [20, 21]. Finally, the apoptotic effector protein-cleaved caspase-3 is activated and cellular apoptosis is induced [22]. In this study, it was found that MMP decreased when HO-8910 cells were treated with HNPG. This was accompanied by reduced expression of bcl-2 protein, increased expression of bax and cleaved caspase-3, and a downregulated ratio of bcl-2/bax, which together suggest that the proliferation inhibition and induced apoptosis might be related to the mitochondrial apoptosis pathway, in which mitochondrial contents are released into the cytoplasm and the caspase family cascade reactions are activated for mitochondrial injury.

In summary, HNPG significantly inhibited proliferation and induced apoptosis of HO-8910 *in vitro*, and the molecular biological mechanism might be closely related to the downregulation of the cellular antioxidant enzyme system. In turn, this downregulation reduced the capacity of scavenging ROS, contributed to ROS accumulation in cells, damaged mitochondrial lipid membrane, reduced cellular MMP, caused mitochondrial dysfunction, released cyt-c and other apoptosis-inducing substances into the cytoplasm, activated the caspase enzyme chain reaction, and resulted in cell apoptosis. However, to determine whether HNPG inhibits the growth and proliferation of ovarian cancer cells *in vivo* and whether HNPG possesses synergistic effects with other traditional anticancer drugs, further study is needed.

Acknowledgments

The authors would like to thank the researchers who worked on Genistein in anti-tumor cells. The authors would also like to thank Professor Wanyu Xie (The First Affiliated Hospital of University of South China, Hengyang, Hunan, China) for her technical assistance.

Funding

Supported by a grant from the Scientific Research Project of Shanxi Provincial Health Commission (No. 2021166).

Conflicts of interest

The authors indicated no potential conflicts of interest.

Author contributions

Yanping Gao and Zhiyong Dong contributed to data acquisition. Jun Bai contributed to data acquisition, data interpretation, and reviewed and approved the final version of this manuscript.

Data availability statement

The data that support the findings of this study are available from the corresponding author upon reasonable request.

Ethical approval

Not applicable.

References

- Okusaka T, Furuse J. Recent advances in chemotherapy for pancreatic cancer: evidence from Japan and recommendations in guidelines. *J Gastroenterol*. 2020;55(4):369-382.
- Feldmann G. Medikamentöse Therapie des Pankreaskarzinoms : Immer noch eine Domäne der Chemotherapie? [Medicinal treatment of pancreatic cancer: Still a domain of chemotherapy?]. *Internist (Berl)*. 2020;61(2):226-232. German.
- Jaiswal N, Akhtar J, Singh SP, Badruddeen, Ahsan F. An overview on genistein and its various formulations. *Drug Res (Stuttg)*. 2019;69(6):305-313.
- Ardito F, Di Gioia G, Pellegrino MR, et al. Genistein as a potential anticancer agent against head and neck squamous cell carcinoma. *Curr Top Med Chem*. 2018;18(3):174-181.
- Bai J, Luo X. 5-Hydroxy-4'-Nitro-7-Propionyloxy-Genistein Inhibited Invasion and Metastasis via Inactivating Wnt/b-Catenin Signal Pathway in Human Endometrial Carcinoma Ji Endometrial Cells. *Med Sci Monit*. 2018;24:3230-3243.
- Bai J, Yang BJ, Luo X. Effects of 5-hydroxy-4'-nitro-7-propionyloxy-genistein on inhibiting proliferation and invasion via activating reactive oxygen species in human ovarian cancer A2780/DDP cells. *Oncol Lett*. 2018;15(4):5227-5235.
- Brioude F, Toutain A, Giabicani E, et al. Overgrowth syndromes - clinical and molecular aspects and tumour risk. *Nat Rev Endocrinol*. 2019;15(5):299-311.
- D'Arcy MS. Cell death: a review of the major forms of apoptosis, necrosis and autophagy. *Cell Biol Int*. 2019;43(6):582-592.
- Spencer SH, Menard SM, Labeled MZ, et al. Enteral tube administration of oral chemotherapy drugs. *J Oncol Pharm Pract*. 2020;26(3):703-717.
- Foster CH, Dave P, Sherman JH. Chemotherapy for the management of cerebral metastases. *Neurosurg Clin N Am*. 2020;31(4):603-611.
- Nada HA, El-Shabrawy MM, Ibrahim SH, et al. Measurement of serum glutathione peroxidase, catalase and superoxide dismutase concentration in patients with external anogenital warts before and after treatment with intralesional tuberculin purified protein derivative. *Andrologia*. 2020;52(9):e13661.
- Pudlarz AM, Czechowska E, S Karbownik M, et al. The effect of immobilized antioxidant enzymes on the oxidative stress in UV-irradiated rat skin. *Nanomedicine (Lond)*. 2020; 15(1):23-39.
- Chen R, Zhu Q, Fang Z, et al. Aluminum induces oxidative damage in *Saccharomyces cerevisiae*. *Can J Microbiol*. 2020;66(12):713-722.
- Tatar Ş, Türkmenoğlu Y. Investigation of antioxidant responses in *Gammarus pulex* exposed to Bisphenol A. *Environ Sci Pollut Res Int*. 2020;27(11):12237-12241.
- Cui N, Pozzobon V, Guerin C, et al. Effect of increasing oxygen partial pressure on *Saccharomyces cerevisiae* growth and antioxidant and enzyme productions. *Appl Microbiol Biotechnol*. 2020;104(18):7815-7826.
- Habashy WS, Milfort MC, Rekaya R, et al. Cellular antioxidant enzyme activity and biomarkers for oxidative stress are affected by heat stress. *Int J Biometeorol*. 2019;63(12):1569-1584.
- Edlich F. BCL-2 proteins and apoptosis: Recent insights and unknowns. *Biochem Biophys Res Commun*. 2018;500(1):26-34.
- Cui L, Bu W, Song J, et al. Apoptosis induction by alantolactone in breast cancer MDA-MB-231 cells through reactive oxygen species-mediated mitochondrion-dependent pathway. *Arch Pharm Res*. 2018;41(3):299-313.
- Senichkin VV, Pervushin NV, Zuev AP, et al. Targeting Bcl-2 family proteins: What, Where, When? *Biochemistry (Mosc)*. 2020;85(10):1210-1226.
- Chea EE, Deredge DJ, Jones LM. Insights on the conformational ensemble of Cyt C reveal a compact state during peroxidase activity. *Biophys J*. 2020;118(1):128-137.
- Barayeu U, Lange M, Méndez L, et al. Cytochrome c autocatalyzed carbonylation in the presence of hydrogen peroxide and cardiolipins. *J Biol Chem*. 2019;294(6):1816-1830.
- Hentzen NB, Mogaki R, Otake S, et al. Intracellular photoactivation of caspase-3 by molecular glues for spatiotemporal apoptosis induction. *J Am Chem Soc*. 2020;142(18):8080-8084.

DOI 10.1007/s10330-022-0596-6

Cite this article as: Gao YP, Dong ZY, Bai J. A novel derivative of Genistein inhibits proliferation of ovarian cancer HO-8910 cells by regulating reactive oxygen species. *Oncol Transl Med*. 2022;8(6): 285–292.